

# Non-homogeneous approximation for the kurtosis evolution of shoaling rogue waves

Saulo Mendes<sup>1,2,\*</sup> and Jérôme Kasparian<sup>1,2,†</sup>

<sup>1</sup>*Group of Applied Physics, University of Geneva, 1205 Geneva, Switzerland*

<sup>2</sup>*Institute for Environmental Sciences, University of Geneva, 1205 Geneva, Switzerland*

Bathymetric changes have been experimentally shown to affect the occurrence of rogue waves. We recently derived a non-homogeneous correction to the spectral analysis, allowing to describe the evolution of the rogue wave probability over a shoal. Here, we extend this work to the evolution of the excess kurtosis of the surface elevation, that plays a central role in estimating rare event probabilities. Furthermore, we provide an upper bound to the excess kurtosis. In intermediate and deep water regimes, a shoal does not affect wave steepness nor bandwidth significantly, so that the vertical asymmetry between crests and troughs, the excess kurtosis, and the exceedance probability of wave height stay rather constant. In contrast, in shallower water, a sharp increase in wave steepness increases the vertical asymmetry, resulting in a growth of both the tail of the exceedance probability and the excess kurtosis.

## I. INTRODUCTION

Ocean wave statistics is at the crossroads of ocean engineering and physical oceanography. Ocean engineers are commonly concerned with both short-term and long-term wave statistics [1], while the mechanisms responsible for the formation of extreme waves is the focus in physical oceanography [2]. The unexpected observation of the so-called rogue waves (also known as freak waves) over the past decades [3] reignited the cross-disciplinary interest in wave statistics. These waves seemingly “appear from nowhere” [4], and are by statistical definition at least twice taller than the significant wave height. From an engineering perspective, the performance of theoretical probability models at the tail of the wave height distribution measures their practical success and applicability to structure dimensioning.

Applying the signal processing methods of Rice [5], the bulk of surface gravity waves were demonstrated to follow a Rayleigh distribution of heights [6]. Nevertheless, the Rayleigh distribution is unsuited to capture the tail of the distribution in real ocean conditions [7, 8]. On the other hand, nonlinear theories and their associated probability distributions are inaccurate in a wide range of real ocean conditions [9, 10]. These difficulties were realized early on, such that an approach based on the expansion of sums of Gram-Charlier series for a weakly non-Gaussian distribution of the ocean surface [11] has been widely favoured. As reviewed in Tayfun and Alkhalidi [12], the computation of surface elevation, crest and wave height distributions require methodologies that are often computationally burdensome. Naturally, the excess kurtosis became the centre of wave statistics in an attempt to transfer the problem from the probability distribution to the cumulant expansion [13, 14]. The complexity of water wave solutions led to the use of excess kurtosis as a practical alternative to the evaluation of

statistical distributions [15, 16].

Over the past decade, experiments and numerical simulations have been performed to assess the effect of shoaling of irregular waves on the amplification of rogue wave intensity and occurrence [17–23]. Trulsen *et al.* [24] provided experimental data with the broadest set of conditions and widest range of relative water depths. As reviewed in Mendes and Kasparian [25], three complementary theoretical models for the wave statistics have emerged, albeit they tend to focus on either surface elevation [26], crest height [27] or crest-to-trough height statistics [28]. Although the observed probability of exceedance of rogue waves in the experiments of Trulsen *et al.* [24] have been well described by the third model [28], their observed excess kurtosis has not been addressed yet. To fill this gap, we provide an effective extension to the theory of energy density redistribution [28] to describe the evolution of kurtosis of wave trains travelling over a shoal. Because the increase of the vertical asymmetry between crests and troughs is a key ingredient of the amplification of rogue wave probability over a shoal [12, 28], we derive an approximation for this asymmetry as a function of water depth, bandwidth and steepness. Variations in vertical asymmetry in intermediate and deep water regimes ( $k_p h > 0.5$ ) are too small to affect the amplification of rogue waves travelling past a shoal, unless either the spectrum is significantly broad-banded ( $\nu > 0.5$ ) or the steepness is large ( $\varepsilon = H_s/\lambda > 1/10$ ). Accordingly, the resulting upper bound for the vertical asymmetry leads to an upper bound for the excess kurtosis, a key information for dimensioning structures as well as for wave forecast [29].

## II. THEORETICAL CONSIDERATIONS

We first recall the main ideas of the theory of non-homogeneous analysis of water waves travelling over a shoal [28]. Given a velocity potential  $\Phi(x, z, t)$  and surface elevation  $\zeta(x, t)$  of waves travelling over a horizontally variable water depth  $h(x)$ , the average energy density evolving over a shoal described by  $h(x) = h_0 + x\nabla h$

\* saulo.dasilvamendes@unige.ch

† jerome.kasparian@unige.ch

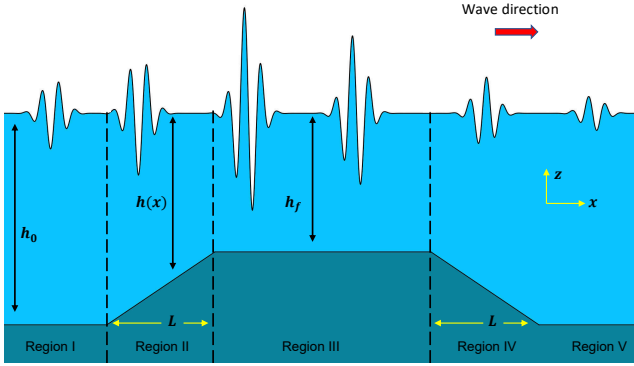


FIG. 1: Portraying of the extreme wave amplification due to a bar [28]. The water column depth evolves as  $h(x) = h_0 + x\nabla h$  with slope  $\nabla h = (h_f - h_0)/L$ . Dashed vertical lines delineate shoaling and de-shoaling regions as in figure 2.

with finite constant slope  $1/20 \leq |\nabla h| < 1$  (see figure 1) is expressed as:

$$\mathcal{E} = \frac{1}{2\lambda} \int_0^\lambda \left\{ \left[ \zeta(x, t) + h(x) \right]^2 - h^2(x) + \frac{1}{g} \int_{-h(x)}^\zeta \left[ \left( \frac{\partial \Phi}{\partial x} \right)^2 + \left( \frac{\partial \Phi}{\partial z} \right)^2 \right] dz \right\} dx, \quad (1)$$

with zero-crossing wavelength  $\lambda$ , gravitational acceleration  $g$  and we abuse the notation for the projection of the gradient of the depth onto the wave direction  $\nabla h \equiv \nabla h \cdot \hat{x} \equiv \partial h / \partial x$ . The inhomogeneity of both  $\mathcal{E}(x)$  and  $\langle \zeta^2 \rangle_t(x)$  redistributes energy among wave heights and transforms their exceedance probability. In the case of an initial Rayleigh distribution in region I of figure 1, over and past the shoal (regions II-V) the exceedance probability reads:

$$\mathbb{P}_{\alpha, \Gamma}(H > \alpha H_s) = \int_\alpha^{+\infty} \frac{4\alpha_0}{\Gamma} e^{-2\alpha_0^2/\Gamma} d\alpha_0 = e^{-2\alpha^2/\Gamma}, \quad (2)$$

where the correction arises from the evolution of an inhomogeneous wave spectrum over the shoal [28] ( $\langle \cdot \rangle_t$  stands for temporal average):

$$\Gamma(x) \approx \frac{\langle \zeta^2(x, t) \rangle_t(x)}{\mathcal{E}(x)}. \quad (3)$$

The spectral correction  $\Gamma$  depends on the steepness  $\varepsilon = H_s/\lambda$  and depth  $k_p h$ , with  $H_s$  being the significant wave height, defined as the average among the 1/3 largest waves. Note that  $H_s$  typically differs by a few percent from its spectral counterpart  $H_{m,0} = 4\sqrt{m_0}$  of Gaussian seas [30, 31], where  $m_0$  is the variance of the surface elevation  $\zeta(x, t)$  computed from the wave spectrum. However, this difference can be as large as 10% in strongly non-Gaussian seas [28, 32]. For linear waves ( $\varepsilon \ll 1/100$ ),  $\Gamma = 1$  and we recover the case of a Gaussian sea. When

solving  $\Gamma$  for second-order irregular waves, we assume that the shoal is linear ( $\nabla^2 h = 0$ ), the length of the shoal is relatively short ( $L/\lambda \lesssim 1$ ) and deal with small amplitude waves only ( $\zeta/h \ll 1$ ). These assumptions greatly simplify the problem, but are also representative of real ocean bathymetry [25]. Furthermore, we have recently demonstrated that as the slope magnitude increases the rogue wave occurrence follows suit. However, if we assume small effect of reflection due to a small surf similarity parameter among spectral components [33], the increase in rogue wave occurrence saturates for slopes larger or equal to  $25^\circ$  [25]. The evolution of the exceedance probability  $\mathbb{P}(H > \alpha H_s)$  in eq. (2) can be generalized to any arbitrary incoming statistics [28]:

$$\ln \left( \frac{\mathbb{P}_{\alpha, \Gamma \mathfrak{E}}}{\mathbb{P}_\alpha} \right) \approx 2\alpha^2 \left( 1 - \frac{1}{\mathfrak{E}^2(\alpha)\Gamma \mathfrak{E}} \right), \quad (4)$$

with the vertical asymmetry between crests and troughs being defined as twice the ratio between crest and crest-to-trough heights [31],

$$\mathfrak{E} = \frac{2Z_c}{H} \quad \therefore \quad 1 \leq \mathfrak{E} \leq 2, \quad (5)$$

which for rogue waves features the mean empirical value:

$$\mathfrak{E}(\alpha = 2) \approx \frac{2\eta_s}{1 + \eta_s} \left( 1 + \frac{\eta_s}{6} \right), \quad (6)$$

where  $\eta_s$  measures the ratio between mean crests and mean troughs and has empirically been found in a wide range of sea conditions to depend on the skewness of the surface elevation  $\mu_3$  [31]:

$$\eta_s \approx 1 + \mu_3. \quad (7)$$

The empirical relations of eqs. (6,7) stem from field observations during North Sea storms detailed in section IV. When the water depth decreases waves become steeper while the super-harmonic contribution has an increasing share of the wave envelope. The combination of these two effects redistributes the exceedance probability by causing the rise in  $\langle \zeta^2 \rangle$  to exceed the growth of  $\mathcal{E}$ . Such uneven growth explains why a shoal in intermediate water amplifies rogue wave occurrence as compared to deep water [24, 34] while it reduces this occurrence in shallow water [35, 36]. The linear term in  $\zeta(x, t)$  has the leading order in deep water and  $\Gamma - 1 \lesssim 10^{-2}$  is small. Conversely, in intermediate water the super-harmonic creates significant disturbances in the energy density increasing  $\Gamma - 1$  up to  $10^{-1}$ , whereas in shallow water the super-harmonic diverges and  $\Gamma - 1 \lesssim 10^{-3}$  becomes small again, reading even smaller values than in deep water.

### III. KURTOSIS EVOLUTION OVER A SHOAL

The probability evolution of eq. (2) depends solely on  $\Gamma$ . Any deviation from a Gaussian distribution may be

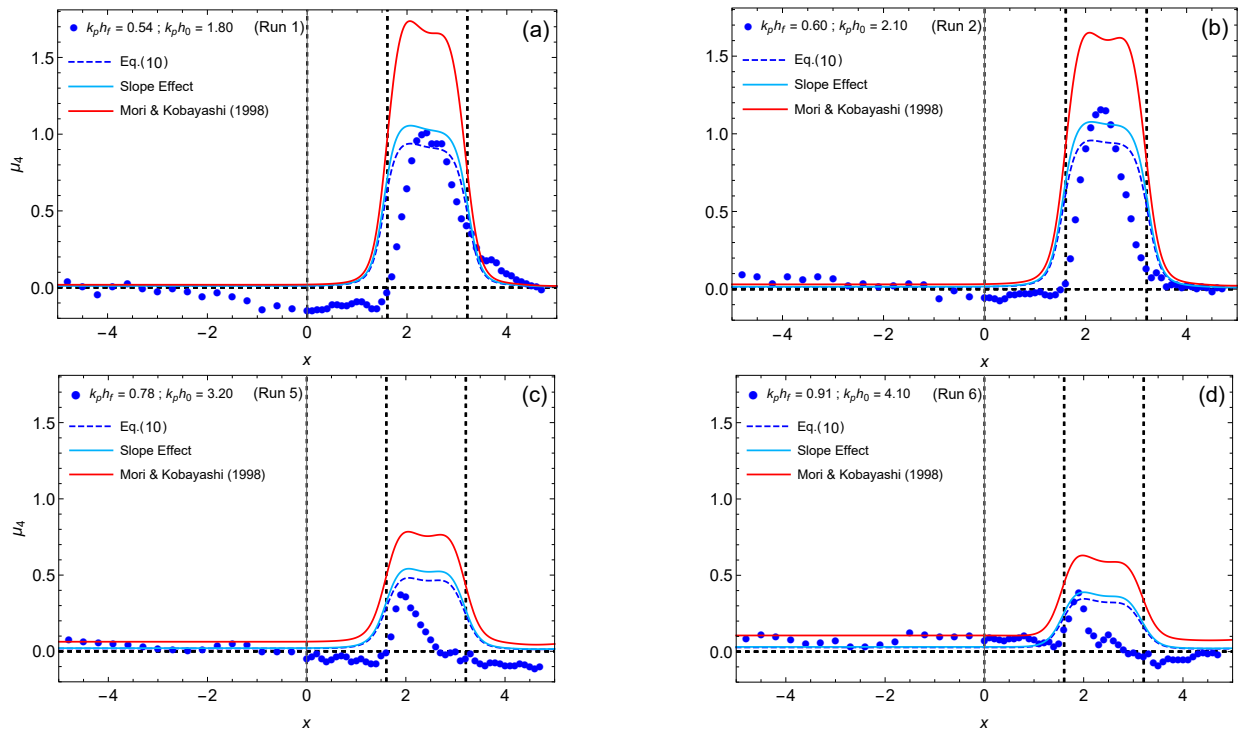


FIG. 2: Observed kurtosis  $\mu_4$  (dots) versus the model of eq. (10) (dashed) for Runs 1, 2, 5, and 6 in Trulsen *et al.* [24]. Dashed vertical lines mark the shoaling and de-shoaling zones (see figure 1). The cyan solid curve includes the slope effect [25] while the red solid curve shows the bound wave prediction according to Mori and Kobayashi [37].

described by a cumulant expansion [11] which at leading order is expressed as a function of the excess kurtosis  $\mu_4$ . For the case of an inhomogeneous wave field due to a shoal, there is an excess in kurtosis due to the energy partition. To avoid the tedious algebra of eqs. (C1,C7b,C12) of Mendes *et al.* [28] for the case of a non-Gaussian sea prior to the shoal, we consider the probability ratio relative to the Rayleigh distribution (implying a pre-shoal  $\mu_4 = 0$ ) to obtain the excess kurtosis. The ratio measures the amplification of the exceedance probability of waves with height  $H = \alpha H_s$  due to a shoal and is computed through the transformation of variables from the wave envelope in Mori and Yasuda [38] into normalized heights to leading order in  $\mu_4$ , as computed in section 6.2.3 of Mendes [39]:

$$\frac{\mathbb{P}_{\alpha, \mu_4}}{\mathbb{P}_\alpha} \approx 1 + \mu_4 \frac{\alpha^2}{2} (\alpha^2 - 1) + \mu_3^2 \frac{5\alpha^2}{18} (2\alpha^4 - 6\alpha^2 - 3), \quad (8)$$

Taking into account the theoretical relation  $\mu_4 \approx 16\mu_3^2/9$  between kurtosis and skewness for waves of second-order in steepness confirmed by wave shoaling experiments [37], we rewrite eq. (8):

$$\frac{\mathbb{P}_{\alpha, \mu_4}}{\mathbb{P}_\alpha} \approx 1 + \mu_4 \cdot \frac{\alpha^2}{32} (10\alpha^4 - 14\alpha^2 - 31), \quad \forall \alpha \gtrsim 2. \quad (9)$$

The kurtosis measures tailness and it affects the exceedance probability for  $\alpha \gtrsim 1.5$ . Eqs. (4) and (9) both describe the same consequence of energy redistribution

and the associated deviation from a Gaussian sea, but the former embodies the physics of shoaling while the latter delineates the perturbation on the statistics regardless of the physical mechanism. Therefore, they can be matched, yielding a kurtosis  $\mu_4(\Gamma, \alpha)$ . This matching could be performed at any value  $\alpha \geq 1.5$ , however, higher accuracy is obtained in the region of stability of the approximation ( $2 \lesssim \alpha \lesssim 3$ ). Over this range, the resulting value of  $\mu_4$  deviates by less than 20%. Therefore, we match both equations at  $\alpha = 2$  without substantial loss in precision:

$$\mu_4(\Gamma) \approx \frac{1}{9} \left[ e^{8(1 - \frac{1}{\alpha^2 \Gamma})} - 1 \right]. \quad (10)$$

This expression generalizes the result obtained by eqs. 46-47 of Mori and Janssen [16] in the case of a narrow-banded wave train, with less than 5% deviation as compared to their model with a  $(2/3)\alpha^2(\alpha^2 - 1)$  polynomial in the counterpart of eq. (9) for small values of the skewness ( $\mu_3 \ll 1$ ). However, if the surface elevation is significantly skewed ( $\mu_3 \gtrsim 1$ ) the contribution of the skewness is severely underpredicted by eqs. 46-47 of Mori and Janssen [16] and therefore the excess kurtosis will be over-predicted while describing the ratio  $\mathbb{P}_{\alpha, \mu}/\mathbb{P}_\alpha$ . In order to validate our effective theory for steep slopes of eq. (10), figure 2 compares its prediction with the observed excess kurtosis in Trulsen *et al.* [24]. In the comparison, we employed the empirical [31] asymmetry  $\mathfrak{S}(\alpha = 2) = 1.2$ . We shall validate this approximation in the next section in

relative water depth  $k_p h \gtrsim \pi/10$ , bandwidth  $\nu \lesssim 1/2$  as defined in Longuet-Higgins [40] and steepness  $\varepsilon \ll 1/10$  representative of Trulsen *et al.*'s experiments. In these experiments, irregular waves with broad-banded JON-SWAP spectrum of  $\gamma = 3.3$  peak enhancement factor, significant wave height  $1.4 \text{ cm} < H_s < 3.4 \text{ cm}$  and peak period  $0.7 \text{ s} < T_p < 1.1 \text{ s}$  were generated in a 24.6 m long and 0.5 m wide unidirectional wave tank. These irregular waves travelled over a flat bottom that had initial relative water depth ranging from  $k_p h = 4.9$  (deep water) to  $k_p h = 1.8$  (intermediate water). Furthermore, the irregular waves propagated over a symmetrical breakwater as sketched in figure 1 with slope  $|\nabla h| \approx 1/3.8$  on each side and located 10.8 m after the wavemaker, or equivalently half a dozen peak wavelengths. The relative water depths atop the shoal are in the range  $0.54 \leq k_p h \leq 1.60$ . In addition, the absolute water depths ranged from 0.5-0.6 m prior to the shoal and from 0.08-0.18 m atop the shoal. Eq. (10) reproduces well the magnitude and the trend of the peak in excess kurtosis to decrease towards deeper waters of the experiments in Trulsen *et al.* [24] (see figure 2). Remaining differences such as the slightly earlier rise of kurtosis in the shoaling zone and the later fall in the de-shoaling zone are likely due to the assumption of negligible reflection. We also computed the kurtosis contribution due to the bound wave following Mori and Kobayashi [37] to evaluate its performance over abrupt changes in relative water depth, see appendix A. This bound kurtosis model (red curve in figure 2) captures the qualitative trend for the observed kurtosis evolution. However, since the latter was developed for a flat bottom and has no explicit slope dependence it overestimates the magnitude of the effect. Furthermore, our model in eq. (10) has the advantage of being extendable to any arbitrary slope [25].

#### IV. VERTICAL ASYMMETRY IN FINITE DEPTH

Eqs. (4) and (10) highlight the influence of the vertical asymmetry on the evolution of rogue wave occurrence and excess kurtosis of the surface elevation over a shoal in intermediate depths. However, the evolution of this asymmetry due to finite depth effects is not well-known, except that it is a slowly varying function of the steepness [12, 41]. To describe the change in vertical asymmetry due to bandwidth and relative water depth, we assess data from North Sea observations. Data was collected on Total Oil Marine's oil platform North Alwyn NAA located at  $60^\circ 48.5' \text{ N}$  and  $1^\circ 44.2' \text{ E}$ , approximately 135 km east of the Shetland Islands (Scotland) and 156 km west of the Norwegian coast [42, 43]. The platform sits on a depth of 129 m and on a mild slope of  $\nabla h \sim -1/300$  in the SE-NW direction (according to bathymetry charts from EMODnet - European Marine Observation and Data Network, see figure 3). While the mean wave direction during the winter storms ob-

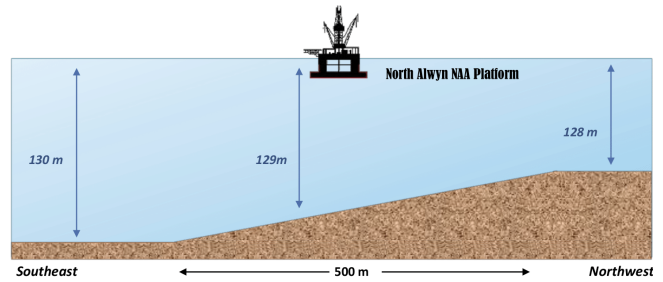


FIG. 3: Approximate bathymetric features around the oil platform in the North Sea. The sketch is not up to scale.

served between 1995-1999 [44] is in the SE-NW direction, we focused on the shoaling case, i.e. waves coming from the southeast towards the northwest. The mild slope is almost linear ( $\nabla^2 h \approx 0$ ) within a distance of 250 m Northwest and Southeast of the platform, corresponding to three mean wavelengths (see table 3 of Mendes *et al.* [31] for the measurements). The raw data were stored as 2381 20-min records of surface elevation measurements recorded with a sampling rate of 5 Hz. To perform the comparison with ocean data, we follow Marthinsen [15] and consider the skewness of the surface elevation to depend solely on relative water depth and wave steepness  $\mu_3 = \mu_3(\varepsilon, k_p h)$ , and consequently identify  $\mathfrak{S}(\mu_3) = \mathfrak{S}(\varepsilon, k_p h)$  for any  $\alpha$  due to eq. (6). We approximate the skewness as (see eq. 19 of Tayfun [41], where  $\mu$  denotes steepness and  $\lambda_3$  the skewness):

$$\begin{aligned} \mu_3(k_p h > \pi) &\approx 3k_1\sigma(1 - \nu\sqrt{2} + \nu^2) \\ &\equiv 3k_1\sigma \cdot \mathfrak{B}(\nu) \approx \frac{\pi}{\sqrt{2}} \varepsilon \mathfrak{B}(\nu) \quad , \quad (11) \end{aligned}$$

where  $H_s = \pi\varepsilon/\sqrt{2}k_p$  and  $k_p$  is the peak wavenumber obtained from the spectral mean wavenumber  $k_1$  through  $k_p \approx (3/4)k_1$  [28] and  $\nu$  is the spectral bandwidth [40]. In deep water ( $k_p h \geq 5$ ), figure 4a shows that the skewness is almost independent of the bandwidth, as expected from eq. (11). On the other hand, as the depth decreases to intermediate waters the ratio  $\mu_3/\varepsilon$  significantly increases and tends to strongly depend on bandwidth. To account for this finite depth effect, we rewrite eq. (11) according to eq. 11 of Tayfun and Alkhalidi [12]:

$$\mu_3 \approx \frac{\pi\varepsilon}{\sqrt{2}} \mathfrak{B}(\nu) \left( \tilde{\chi}_0 + \frac{\sqrt{\tilde{\chi}_1}}{2} \right) \quad , \quad (12)$$

with notation  $\tilde{\chi}_i$  from Mendes *et al.* [28]:

$$\begin{aligned} \tilde{\chi}_0 &= \frac{\left[ 4 \left( 1 + \frac{2k_p h}{\sinh(2k_p h)} \right) - 2 \right]}{\left( 1 + \frac{2k_p h}{\sinh(2k_p h)} \right)^2 \tanh k_p h - 4k_p h} \quad , \\ \frac{\sqrt{\tilde{\chi}_1}}{2} &= \frac{3 - \tanh^2(k_p h)}{2 \tanh^3(k_p h)} \quad . \quad (13) \end{aligned}$$

Although Tayfun and Alkhalidi's model provides a good

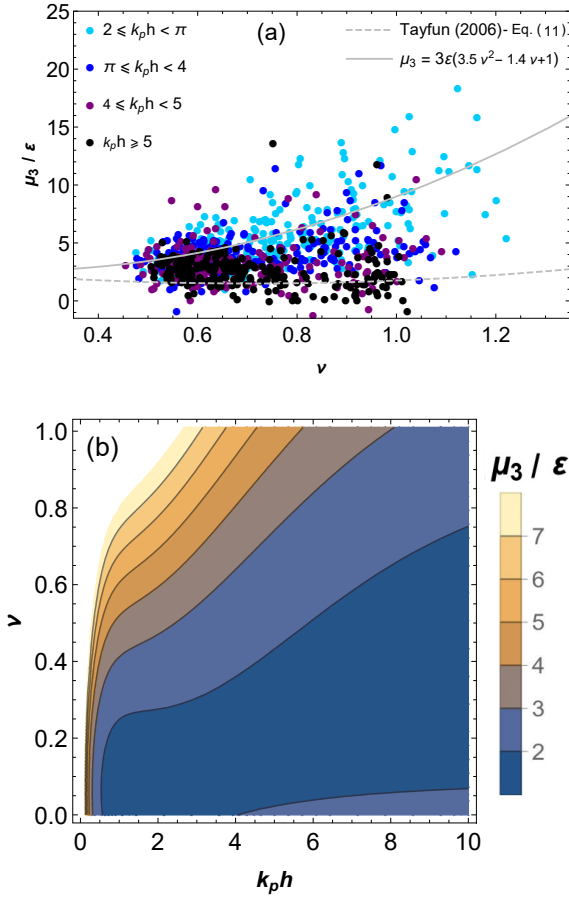


FIG. 4: (a) Ratio of skewness and steepness varying with bandwidth in strongly non-Gaussian ( $\mu_4 \approx 0.4$ ) North Sea data [42], with polynomial fit  $\mathfrak{B}(\nu) \approx 1 - \nu\sqrt{2} + 3.5\nu^2$  at  $2 \leq k_p h \leq \pi$ . (b) Contour plot of the same ratio as computed from eq. (12) for the fitted function  $\mathfrak{B}(\nu, k_p h)$  in (a).

fit of  $\mu_3/\varepsilon$  for  $k_p h > 3$ , the sum  $\tilde{\chi}_0 + \sqrt{\tilde{\chi}_1}/2$  stays close to unity for  $k_p h \geq 2$ . Hence, the larger values of the ratio  $\mu_3/\varepsilon$  for shallower water ( $2 \leq k_p h \leq \pi$ ) must stem from a dependence of  $\mathfrak{B}(\nu)$  with depth. We therefore seek a generalization of eq. (12) whereby we fit a function  $\mathfrak{B}(\nu, k_p h) = 1 - \nu\sqrt{2} + f_{k_p h} \cdot \nu^2$  capable of providing a smooth transition from  $f_{k_p h \sim 3} \approx 3.5$  in shallower depths (see figure 4a) to the deep water value  $f_{k_p h \rightarrow \infty} \sim 1$  (see eq. (11)). Hence, implementing this fit into eqs. (6,7) the vertical asymmetry accounting for depth-induced effects is of the type:

$$\mathfrak{S}(\alpha = 2) \approx \frac{(2 + 6\varepsilon_*)(7 + 3\varepsilon_*)}{6(2 + 3\varepsilon_*)}, \quad (14)$$

where  $\varepsilon_*$  is the effective steepness:

$$\varepsilon_* \approx \frac{\pi\varepsilon}{3\sqrt{2}} \left[ 1 - \nu\sqrt{2} + f_{k_p h} \cdot \nu^2 \right] \left( \tilde{\chi}_0 + \frac{\sqrt{\tilde{\chi}_1}}{2} \right). \quad (15)$$

Figure 4b provides a contour plot for the ratio  $\mu_3/\varepsilon$  taking into account the fitted model of  $f_{k_p h}$ . Here,  $f_{k_p h}$  is

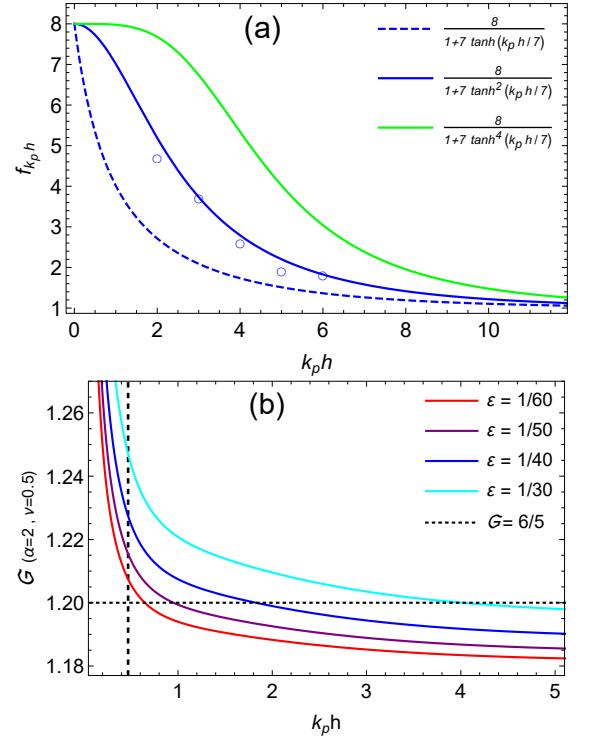


FIG. 5: (a) Finite-depth functions  $f_{k_p h}$  versus data (circles) from figure 4a. (b) Vertical asymmetry of broad-banded rogue waves ( $\nu = 0.5$ ) as a function of water depth for different steepness, with the dotted line depicting the empirical mean value  $\mathfrak{S} = 6/5$  from Mendes *et al.* [28, 31]. Dashed vertical line marks the limit of validity of second-order theory.

a function of depth that can be obtained through the constraint  $\mathfrak{S} \leq 2$  of eq (5) applied to eq. (14):

$$\lim_{k_p h \rightarrow 0} \mathfrak{S}(\alpha = 2) \approx \lim_{k_p h \rightarrow 0} \frac{(2 + 6\varepsilon_*)(7 + 3\varepsilon_*)}{6(2 + 3\varepsilon_*)} \leq 2, \quad (16)$$

thus leading to:

$$9\varepsilon_*^2 + 6\varepsilon_* - 5 \leq 0 \quad \therefore \quad \varepsilon_* \leq \frac{\sqrt{6} - 1}{3}. \quad (17)$$

The function  $\mathfrak{B}(\nu, k_p h)$  makes the exceedance probability of rogue waves weakly dependent on the bandwidth  $\nu$  [40]. Very broad-banded seas ( $\nu \geq 1$ ) are very rare. For example, they account for only 3% of observed stormy states in the North Sea [31]. These extreme sea conditions are typically short-lived and found for instance in hurricanes. Albeit bandwidths much larger than  $\nu = 1$  can increase the vertical asymmetry by about 5-10%, their lifespan impacts the weighted average of the exceedance probability of rogue waves over a daily forecast by only  $\sim 10\%$  because  $\nu \sim 0.5$  over 97% of all 30-min records. Accordingly, we may set  $\nu = 1$  as the realistic and effective maximum bandwidth to be considered for estimating the rogue wave exceedance probabil-

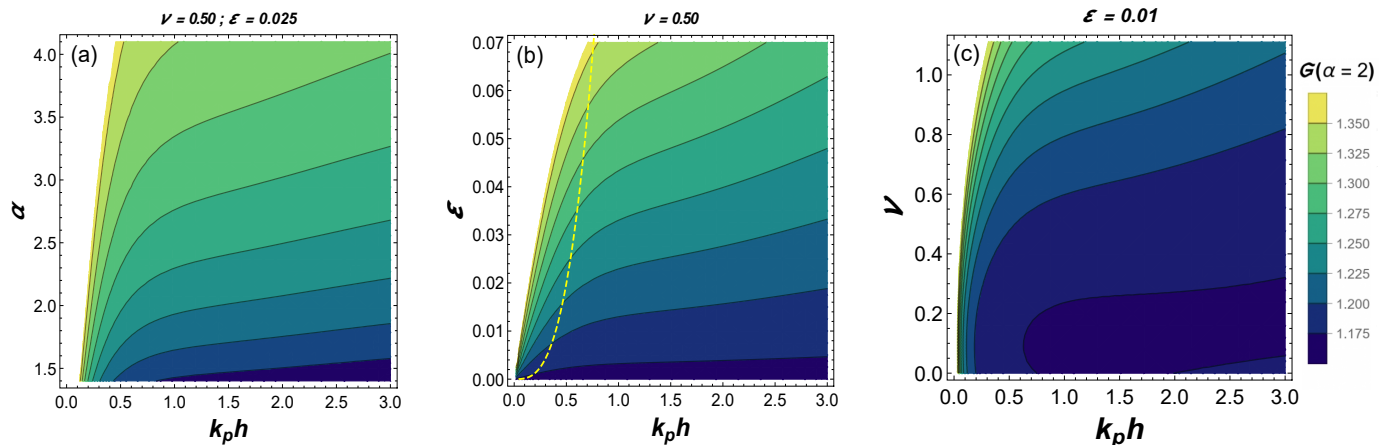


FIG. 6: Vertical asymmetry of large and rogue waves as a function of water depth for different steepness, bandwidth and normalized height. The dashed line in panel b represents the Ursell limit for second-order theory.

ity. Hence, in the second-order limit we obtain:

$$\lim_{k_p h \rightarrow 1/2} \frac{\pi \varepsilon}{3\sqrt{2}} f_{k_p h} \left( \tilde{\chi}_0 + \frac{\sqrt{\tilde{\chi}_1}}{2} \right) < \frac{\sqrt{6} - 1}{3} \quad , \quad (18)$$

Consequently, broad-banded waves will not exceed the following depth correction:

$$f_{k_p h}(\nu = 1) \lesssim \frac{18\sqrt{2}}{\pi} \approx 8 \quad . \quad (19)$$

Broad-banded waves have an effective steepness of the order of  $\varepsilon f_{k_p h} \nu^2$ . Since finite-depth effects involve the ratio  $\varepsilon/k_p h$  which it is directly related to  $H_s/h$  and  $f_{k_p h}$  grows quickly from deep to intermediate waters (see figure 4a), we expect  $f_{k_p h}$  to be inversely proportional to the relative depth  $k_p h$ . In order to fulfill eqs. (16-19), a sigmoid function provides a good fit with continuous derivative for the North Sea data (see figure 5a):

$$f_{k_p h} \approx \frac{8}{1 + 7 \tanh^2(k_p h/7)} \quad , \quad \nu \leq 1 \quad . \quad (20)$$

Plugging eq. (20) into eq. (14) introduces an approximation for the vertical asymmetry covering the entire range of second-order theory for narrow and broad-banded irregular waves. In fact, figure 5b shows that the vertical asymmetry is almost constant for typical values of mean steepness ( $\varepsilon \ll 1/10$ ) in intermediate and deep waters ( $k_p h \geq \pi/10$ ). Conversely, sharp increases in the mean steepness will induce a few percent increase in the vertical asymmetry in the same regimes ( $k_p h \geq \pi/10$ ). The contour plot in figure 6b provides a full description of the variations in asymmetry with depth and steepness. Furthermore, figure 6a shows that in shallow depths the vertical asymmetry strongly depends on  $k_p h$  while in deep water it tends to saturate. Figure 6c also illustrates the role of bandwidth in increasing the asymmetry, albeit sharp changes are restricted to sufficiently broad spectra ( $\nu > 0.8$ ). Thus, the analysis of field data from the North

Sea shows that as long as the steepness in intermediate water ( $k_p h > \pi/10$ ) is small ( $\varepsilon < 1/10$ ) or the spectrum narrow ( $\nu < 1/2$ ), the vertical asymmetry stays close to  $\mathfrak{S} = 1.2$ . We find this approximation for the vertical asymmetry to be still applicable to the experiments in Trulsen *et al.* [24] with steeper slope, as shown in appendix B.

Moreover, the special case of narrow-banded ( $\nu = 0$ ) linear waves ( $\varepsilon \ll 1/10$ ) in deep water leads to  $\varepsilon_* \rightarrow 0$ , thus reaching the lower bound of the asymmetry  $\mathfrak{S} = 7/6$  for rogue waves. This suggests that in intermediate waters narrowing the bandwidth from  $\nu = 0.3$  to  $\nu = 0$  will have little impact on the amplification of rogue wave statistics due to the negligible change in vertical asymmetry, whereas in shallow water increasing the bandwidth above  $\nu = 0.5$  will significantly boost rogue wave occurrence. From the point of view of the theory in Mendes *et al.* [28], the asymmetry approximation of eqs. (14,20) explains why narrow-banded models [27] are successful in predicting rogue wave statistics travelling past a step in a broad-banded irregular wave background in intermediate water. Provided there is no wave breaking ( $H_s/h \ll 1$ ), the bandwidth effect will play a role in amplifying statistics in shallower depths because of the contribution of the term  $f_{k_p h} \nu^2$ , as experimentally demonstrated in Doleman [45].

## V. UPPER BOUND FOR KURTOSIS

The excess kurtosis has been used in the past two decades as a proxy for how rough nonlinear seas increase the occurrence and intensity of rogue waves. Therefore, in this section we extend our results of section III to estimate the maximum kurtosis atop any shoal in the ocean [29, 46]. The assessment of maximum expected waves over a specific return time at a fixed location is crucial for naval design. Typically, ocean structures and vessels must be designed to sustain expected maximum

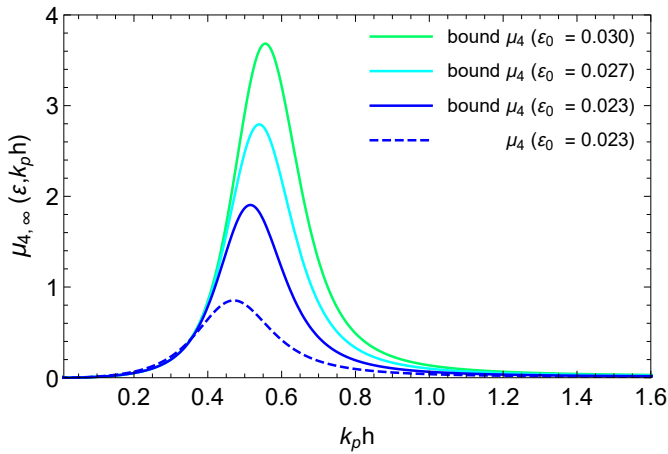


FIG. 7: Upper bound on kurtosis from eq. (23) for  $\nu = 0.5$  and different pre-shoal steepness  $\epsilon_0$  subject to linear shoaling. The dashed curve represents the computed kurtosis in figure 2a, representative of Run 1 of Trulsen *et al.* [24].

extreme waves over their lifespan [47, 48]. In order to do so, we shall evaluate maxima for the parameters  $\mathfrak{S}$  and  $\Gamma$ . Eqs. (14) and (20) provide the upper bound for the vertical asymmetry of rogue waves in the limit of wave breaking:  $\mathfrak{S}_\infty(k_p h = \infty) \approx 1.387$  in deep water and  $\mathfrak{S}_\infty(k_p h = 0) \approx 1.668$  in shallow water. Since the  $\Gamma$  correction is also limited by wave breaking, one finds the bound  $\Gamma_\infty - 1 \lesssim 1/12$  due to eq. (3.17) of Mendes *et al.* [28]. Hence, we may approximate:

$$1 - \frac{1}{\mathfrak{S}_\infty^2 \Gamma_\infty} \lesssim 8(\Gamma_\infty - 1) \quad . \quad (21)$$

Approaching the value  $\Gamma_\infty$  atop the shoal (region III of figure 1), the contribution of the skewness to the amplification of wave statistics near the breaking regime increases such that the relationship between kurtosis and skewness leading to eq. (9) is modified and now empirically reduces to  $\mu_4 \approx \mu_3^2$  [19]. Plugging this relationship into eq. (8) and comparing it with eqs. (4,21), we obtain:

$$e^{16\alpha^2(\Gamma_\infty - 1)} \geq 1 + \alpha^2 (\alpha^2 - 1) \mu_4 \quad . \quad (22)$$

At  $\alpha = 2$ , the evaluation of the excess kurtosis lies at the region of stability of the Gram-Charlier series and we are able to compute the upper bound for the excess kurtosis in the case of a pre-shoal Gaussian statistics (see figure 7):

$$\mu_{4, \infty} \approx \frac{1}{12} \left[ e^{64(\Gamma_\infty - 1)} - 1 \right] \quad , \quad (23)$$

where  $\Gamma_\infty$  varies with water depth. According to eq. (23), typical seas with steep and highly asymmetrical broad-banded waves lead to an upper bound for the excess kurtosis of the order of  $\mu_{4, \infty} \sim 4$  in intermediate water, see figure 7. We already described that the maximum value

of  $\Gamma$  is located around  $k_p h \approx 0.5$  in Mendes *et al.* [28] and eq. (10) has been validated in figure 2. Therefore, the peak in excess kurtosis will also be located in this region. Experiments conducted in Zhang *et al.* [49] found the peak in excess kurtosis in the same region  $k_p h \approx 0.5$ .

## VI. CONCLUSIONS

In this work we have extended the framework in Mendes *et al.* [28] to an effective theory for the evolution of excess kurtosis of the surface elevation over a shoal of finite and constant steep slope. We find quantitative agreement with experiments in Trulsen *et al.* [24] regarding the magnitude of the kurtosis increase during and atop the shoal. While the groundwork of Marthinsen [15] computes the excess kurtosis directly from the solution  $\zeta(x, t)$ , our model unravels the kurtosis dependence on the inhomogeneities of the energy density over a shoal. Our formulation outperforms the conventional method of Marthinsen [15] for the computation of kurtosis of the bound wave contribution. In addition, our effective theory is capable of describing changes of the kurtosis magnitude over arbitrary slopes provided reflection can be neglected. A computation of the kurtosis from the probability density of  $\zeta(x, t)$  through the non-homogeneous framework will be pursued in a future work with an analytical non-uniform distribution of random phases.

Furthermore, we have obtained an approximation for the vertical asymmetry in finite depth as a function of both steepness and bandwidth. This approximation extends the seminal work of Tayfun [41] for the skewness of the surface elevation to broad-banded intermediate water waves while recovering its original formulation for narrow-banded deep water waves. Building on this new approximation, we have demonstrated that the vertical asymmetry varies slowly over a shoal in both deep and intermediate waters. Moreover, based on this rise in vertical asymmetry we were able to compute an upper bound for the excess kurtosis driven by shoaling.

## VII. ACKNOWLEDGMENTS

S.M and J.K. were supported by the Swiss National Science Foundation under grant 200020-175697. We thank Maura Brunetti and Alexis Gomel for fruitful discussions.

### Appendix A: Computation of Irregular Bound Wave Kurtosis

The contribution of bound waves to the excess kurtosis of the surface elevation is given by Mori and Kobayashi

[37] in the regular wave approximation:

$$\mu_4 = 3 \left\{ \frac{1 + (ka)^2(6D_1^2 + 6D_2^2 + 8D_1D_2)}{[1 + (ka)^2(D_1^2 + D_2^2)]^2} - 1 \right\}, \quad (\text{A1})$$

where  $D_1$  and  $D_2$  are relative water depth coefficients from the surface elevation:

$$D_1 = \frac{1}{\tanh kh}; \quad D_2 = D_1 \left( 1 + \frac{3}{2 \sinh^2 kh} \right). \quad (\text{A2})$$

To leading order in steepness, we may approximate the excess kurtosis as:

$$\begin{aligned} \mu_4 &\approx 3 \left\{ \left[ 1 + (ka)^2(6D_1^2 + 6D_2^2 + 8D_1D_2) \right] \right. \\ &\quad \times \left. \left[ 1 - 2(ka)^2(D_1^2 + D_2^2) \right] - 1 \right\}, \\ &\approx 3 \left\{ \left[ 1 + (ka)^2(4D_1^2 + 4D_2^2 + 8D_1D_2) \right] - 1 \right\}, \\ &\approx 3(ka)^2(4D_1^2 + 4D_2^2 + 8D_1D_2) \\ &\approx 12(ka)^2(D_1 + D_2)^2, \end{aligned} \quad (\text{A3})$$

However, we shall extend eq. (A1) for irregular waves, computing the equivalent irregular mean wave steepness and relative depth. We may use  $ka \rightarrow k_p H_s / 2\sqrt{2}$  as pointed out in Trulsen *et al.* [24] for irregular waves, consequently we find  $ka \rightarrow (\pi/4)\varepsilon$  as in Mendes *et al.* [28]. Hence, we may write the excess kurtosis as a function of  $\varepsilon$  up to second order in steepness:

$$\mu_4 \approx \frac{3\pi^2}{4} \cdot \varepsilon^2 (D_1 + D_2)^2. \quad (\text{A4})$$

Moreover, the depth  $kh$  has to be converted to its peak wavenumber equivalent  $k_p h$ . Hence, since observations in the ocean feature  $1.1 \leq \lambda_p / \lambda_{1/3} \leq 1.2$  [50], we may use the transformation from regular wave to irregular wave  $kh \rightarrow 1.2k_p h$  to compute  $(D_1, D_2)$  correctly. As a remark, the above expression differs little from formulations such as of Marthinsen [15] and others as reviewed in Tayfun and Alkhalidi [12].

## Appendix B: Slope Effect on Vertical Asymmetry

In this section we assess how the vertical asymmetry of irregular rogue waves is affected by an arbitrary slope. Let us denote the final steepness atop the shoal as  $\varepsilon_f$  and the initial one as  $\varepsilon_0$ . If linear waves travel over a shoal, then we may define the amplification ratio of the steepness (also known as shoaling coefficient):

$$K_{\varepsilon, L} := \frac{\varepsilon_f}{\varepsilon_0} \approx \frac{1}{\tanh(1.2k_p h)} \left[ \frac{2 \cosh^2(1.2k_p h)}{2.4k_p h + \sinh(2.4k_p h)} \right]^{1/2}, \quad (\text{B1})$$

where we have converted the regular wave formula [51] to irregular waves. Indeed, except for a few percent,

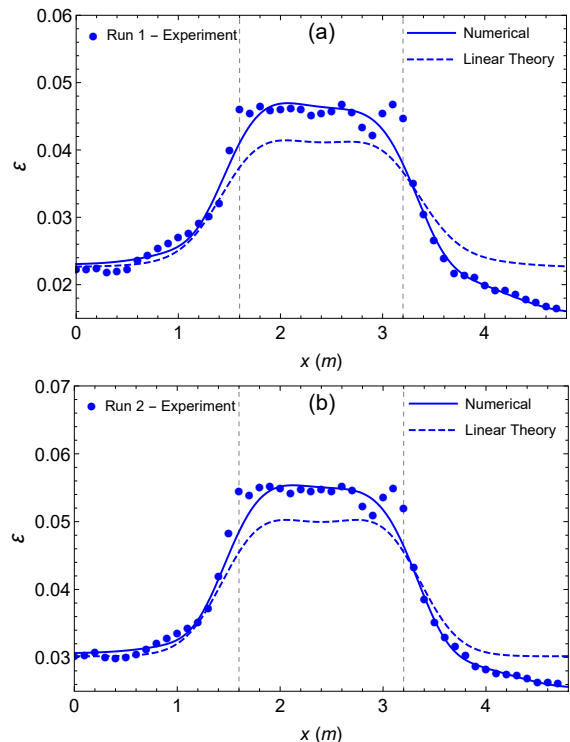


FIG. 8: Theoretical evolution of steepness measured against observations (dots) in Raustøl [18] and its numerical fit thereof for (a) Run 1 and (b) Run 2 of the experiments in Trulsen *et al.* [24].

the shoaling coefficient of the (irregular) significant wave height is a good approximation for the regular wave counterpart [52, 53]. If nonlinear wave shoaling is dominant, then  $K_{\varepsilon, NL}$  depends on the slope of the shoal  $\nabla h$ , and we denote the ratio  $K_{\varepsilon, NL} / K_{\varepsilon, L} = \mathcal{F}_{\nabla h}$  [54–56]. Performing a Taylor expansion in eq. (14) up to first order in  $\varepsilon_*$ , the vertical asymmetry of small wave amplitudes can be written as:

$$\mathfrak{G}(\alpha = 2) \approx \frac{7}{6}(1 + 2\varepsilon_*) \quad (\text{B2})$$

The typical sea representative of Trulsen *et al.* [24] experiments is broad-banded ( $\nu \sim 0.5$ ) and in intermediate water ( $k_p h \sim 1$ ). Recalling eqs. (15,20), this leads to  $\mathfrak{B}(\nu) \sim 2$  and  $\tilde{\chi}_0 + \sqrt{\tilde{\chi}_1}/2 \sim 1$ . Therefore we may approximate  $\varepsilon_* \approx (\pi\sqrt{2}/3)\varepsilon$ . Consequently, the ratio between the vertical asymmetry of identical sea states of waves travelling over a shoal of different slopes is approximately described by the formula:

$$\frac{\mathfrak{G}_{|\nabla h|}}{\mathfrak{G}} \approx \frac{\left( 1 + \frac{2\sqrt{2}\pi}{3}\varepsilon \cdot \mathcal{F}_{\nabla h} \right)}{\left( 1 + \frac{2\sqrt{2}\pi}{3}\varepsilon \right)} \approx 1 + \frac{2\sqrt{2}\pi}{3}\varepsilon (\mathcal{F}_{\nabla h} - 1). \quad (\text{B3})$$

Even for relatively steep shoals ( $|\nabla h| \approx 1/4$ ) as in the case of Trulsen *et al.* [24] the correction accounting for slope is small, with  $\mathcal{F}_{\nabla h} \approx 1.15$  in this case (see figure



8a,b). In fact, Srineash and Murali [56] demonstrated experimentally that  $\mathcal{F}_{\nabla h} - 1$  stays in the range of 0.1–0.2 for steep slopes. Since the steepness in the experiments of Trulsen *et al.* [24] atop the shoal does not exceed  $\varepsilon = 0.06$ , the slope correction to the vertical asymmetry derived

with the help of field data from the North Sea stay below  $(\pi\sqrt{2}/9) \times 100\% \times 0.06 = 3\%$ . Thus, eq. (14) is applicable to the analysis in section III, and the approximation  $\mathfrak{S} \approx 1.2$  is applicable in the conditions of the experiments in Trulsen *et al.* [24].

- 
- [1] G. Clauss, Dramas of the sea: episodic waves and their impact on offshore structures, *App. Ocean Res.* **24**, 147 (2002).
- [2] A. Toffoli, T. Waseda, H. Houtani, L. Cavaleri, D. Greaves, and M. Onorato, Rogue waves in opposing currents: an experimental study on deterministic and stochastic wave trains, *Journal of Fluid Mechanics* **769**, 277–297 (2015).
- [3] S. Haver, A possible freak wave event measured at the draupner jacket january 1 1995, *Proc. Rogue Waves 20-22 October IFREMER* (2004).
- [4] N. Akhmediev, A. Ankiewicz, and M. Taki, Waves that appear from nowhere and disappear without a trace, *Phys. Lett. A* **373**, 675 (2009).
- [5] S. Rice, Mathematical analysis of random noise, *Bell Syst. Tech. J.* **24**, 46 (1945).
- [6] M. Longuet-Higgins, On the statistical distribution of the heights of sea waves, *Journal of Marine Research* **11**, 245 (1952).
- [7] G. Forristall, On the distributions of wave heights in a storm, *J. Geophys. Res.* **83**, 2353 (1978).
- [8] M. A. Tayfun, Narrow-band nonlinear sea waves, *J. Geophys. Res.* **85**, 1548 (1980).
- [9] I. Karpadakis, C. Swan, and M. Christou, Assessment of wave height distributions using an extensive field database, *Coastal Eng.* **157** (2020).
- [10] I. Teutsch, R. Weisse, J. Moeller, and O. Krueger, A statistical analysis of rogue waves in the southern north sea, *Natural Hazards and Earth System Sciences* **20**, 2665 (2020).
- [11] M. Longuet-Higgins, The effect of non-linearities on statistical distributions in the theory of sea waves, *J. Fluid Mech.* **17**, 459 (1963).
- [12] M. A. Tayfun and M. A. Alkhalidi, Distribution of sea-surface elevations in intermediate and shallow water depths, *Coastal Eng.* **157** (2020).
- [13] E. M. Bitner, Non-linear effects of the statistical model of shallow-water wind waves, *Applied Ocean Research* **2**, 63 (1980).
- [14] M. Tayfun, Distribution of large wave heights, *J. Waterway, Port, Coastal Ocean Eng.* **116**, 686 (1990).
- [15] T. Marthinsen, On the statistics of irregular second-order waves, Report No. RMS-11 (1992).
- [16] N. Mori and P. Janssen, On kurtosis and occurrence probability of freak waves, *J. Phys. Oceanogr.* **36**, 1471 (2006).
- [17] K. Trulsen, H. Zeng, and O. Gramstad, Laboratory evidence of freak waves provoked by non-uniform bathymetry, *Phys. Fluids* **24** (2012).
- [18] A. Raustøl, Freake bølger over variabelt dyp, Master’s thesis, University of Oslo (2014).
- [19] Y.-X. Ma, X.-Z. Ma, and G.-H. Dong, Variations of statistics for random waves propagating over a bar, *Journal of Marine Science and Technology (Taiwan)* **23**, 864 (2015).
- [20] G. Ducrozet and M. Gouin, Influence of varying bathymetry in rogue wave occurrence within unidirectional and directional sea-states, *Journal of Ocean Engineering and Marine Energy* **3** (2017).
- [21] C. Bolles, K. Speer, and M. Moore, Anomalous wave statistics induced by abrupt depth change, *Physical Review Fluids* **4** (2019).
- [22] J. Zhang, M. Benoit, O. Kimmoun, A. Chabchoub, and H.-C. Hsu, Statistics of extreme waves in coastal waters: Large scale experiments and advanced numerical simulations, *Fluids* **4** (2019).
- [23] Y. Li, Y. Zheng, Z. Lin, T. A. Adcock, and T. Van Den Bremer, Surface wavepackets subject to an abrupt depth change. part 1: Second-order theory, *J. Fluid Mech.* **915**, A71 (2021).
- [24] K. Trulsen, A. Raustøl, S. Jorde, and L. Rye, Extreme wave statistics of long-crested irregular waves over a shoal, *J. Fluid Mech.* **882** (2020).
- [25] S. Mendes and J. Kasparian, Saturation of rogue wave amplification over steep shoals, *Phys. Rev. E* **106**, 065101 (2022).
- [26] N. Moore, C. Bolles, A. Majda, and D. Qi, Anomalous waves triggered by abrupt depth changes: Laboratory experiments and truncated kdv statistical mechanics, *Journal of Nonlinear Science* **30**, 3235 (2020).
- [27] Y. Li, S. Draycott, Y. Zheng, Z. Lin, T. Adcock, and T. Van Den Bremer, Why rogue waves occur atop abrupt depth transitions, *Journal of Fluid Mechanics* **919**, R5 (2021).
- [28] S. Mendes, A. Scotti, M. Brunetti, and J. Kasparian, Non-homogeneous model of rogue wave probability evolution over a shoal, *J. Fluid Mech.* **939**, A25 (2022).
- [29] P. E. M. Janssen and J.-R. Bidlot, *On the extension of the freak wave warning system and its verification* (European Centre for Medium-Range Weather Forecasts Reading, UK, 2009).
- [30] M. Casas-Prat and L. Holthuijsen, Short-term statistics of waves observed in deep water, *J. Geophys. Res. Oceans* **115** (2010).
- [31] S. Mendes, A. Scotti, and P. Stansell, On the physical constraints for the exceeding probability of deep water rogue waves, *Appl. Ocean Res.* **108**, 102402 (2021).
- [32] Y. Goda, A unified nonlinearity parameter of water waves, *Rept. Port and Harbour Res. Inst.* **22** (3), 3 (1983).
- [33] J. Battjes, Surf similarity, *Coastal Engineering Proceedings* **1**, 26 (1974).
- [34] O. Kimmoun, H.-C. Hsu, N. Hoffmann, and A. Chabchoub, Experiments on uni-directional and nonlinear wave group shoaling, *Ocean Dynamics* (2021).
- [35] B. K. Glukhovskiy, Investigation of sea wind waves (in russian), *Gidrometeoizdat, Leningrad*, , 283 (1966).

- [36] I. Karmpadakis, C. Swan, and M. Christou, A new wave height distribution for intermediate and shallow water depths, *Coastal Engineering* **175**, 104130 (2022).
- [37] N. Mori and N. Kobayashi, Nonlinear distribution of neashore free surface and velocity, in *Coastal Engineering 1998* (1998) pp. 189–202.
- [38] N. Mori and T. Yasuda, A weakly non-gaussian model of wave height distribution random wave train, *Ocean Eng.* **29**, 1219–1231 (2002).
- [39] S. Mendes, On the statistics of oceanic rogue waves in finite depth: Exceeding probabilities, physical constraints and extreme value theory, UNC Chapel Hill PhD Thesis (2020).
- [40] M. S. Longuet-Higgins, On the joint distribution of the periods and amplitudes of sea waves, *J. Geophys. Res.* **80**, 2688 (1975).
- [41] M. Tayfun, Statistics of nonlinear wave crests and groups, *Ocean Eng.* **33**, 1589 (2006).
- [42] P. Stansell, Distribution of freak wave heights measured in the north sea, *Appl. Ocean Res.* **26**, 35 (2004).
- [43] P. Stansell, Distributions of extreme wave, crest and trough heights measured in the north sea, *Ocean Eng.* **32**, 1015 (2005).
- [44] B. Linfoot, P. Stansell, and J. Wolfram, On the characteristics of storm waves, *Proceedings of the International Offshore and Polar Engineering Conference* **3**, 74 (2000).
- [45] M. W. Doeleman, Rogue waves in the dutch north sea, Master's thesis, TU Delft (2021).
- [46] P. A. E. M. Janssen, *Shallow-water version of the freak wave warning system* (European Centre for Medium Range Weather Forecasts, 2017).
- [47] L. E. Borgman, Probabilities for highest wave in hurricane, *Journal of the Waterways, Harbors and Coastal Engineering Division* **99**, 185 (1973).
- [48] L. R. Muir and A. El-Shaarawi, On the calculation of extreme wave heights: a review, *Ocean Engineering* **13**, 93 (1986).
- [49] J. Zhang, Y. Ma, T. Tan, G. Dong, and M. Benoit, Enhanced extreme wave statistics of irregular waves due to accelerating following current over a submerged bar, *J. Fluid Mech.* **954**, A50 (2023).
- [50] A. Figueras, Estimation of available wave power in the near shore area around hanstholm harbor, Project of Special Thesis, Universidad Politecnica de Catalunya (2010).
- [51] L. H. Holthuijsen, *Waves in Oceanic and Coastal Waters* (Cambridge University Press, 2007).
- [52] Y. Goda, Irregular wave deformation in the surf zone, *Coastal Engineering in Japan* **18**, 13 (1975).
- [53] Y. Goda, *Random seas for design of maritime structures*, World Scientific (2010).
- [54] P. S. Eagleson, Properties of shoaling waves by theory and experiment, *Eos, Transactions American Geophysical Union* **37**, 565 (1956).
- [55] J. Walker and J. Headlam, Engineering approach to nonlinear wave shoaling, *Proceedings of the Coastal Engineering Conference* **1**, 523 (1983).
- [56] V. Srineash and K. Murali, Wave shoaling over a submerged ramp: An experimental and numerical study, *Journal of Waterway, Port, Coastal and Ocean Engineering* **144** (2018).